Noiseless imaging detector for adaptive optics with kHz frame rates

John Vallerga[*a], Jason McPhate[a], Bettina Mikulec[b], Anton Tremsin[a], Allan Clark[b] and Oswald Siegmund[a]
[a]Space Sciences Laboratory, 7 Gauss Way, Univ. of California, Berkeley, CA USA 94720-7450;
[b]University of Geneva, 24, quai Ernest-Ansermet, 1211 Geneva 4, Switzerland

ABSTRACT

A new hybrid optical detector is described that has many of the attributes desired for the next generation AO wavefront sensors. The detector consists of a proximity focused MCP read out by four multi-pixel application specific integrated circuit (ASIC) chips developed at CERN ("Medipix2,,) with individual pixels that amplify, discriminate and count input events. The detector has 512 x 512 pixels, zero readout noise (photon counting) and can be read out at 1kHz frame rates. The Medipix2 readout chips can be electronically shuttered down to a temporal window of a few microseconds with an accuracy of 10 nanoseconds. When used in a Shack-Hartman style wavefront sensor, it should be able to centroid approximately 5000 spots using 7 x7 pixel sub-apertures resulting in very linear, off-null error correction terms. The quantum efficiency depends on the optical photocathode chosen for the bandpass of interest. A three year development effort for this detector technology has just been funded as part of the first Adaptive Optics Development Program managed by the National Optical Astronomy Observatory.

Keywords: adaptive optics, wavefront sensors, MCP, Medipix, GaAs photocathodes

1. INTRODUCTION

The white paper entitled "A Roadmap for the Development of Astronomical Adaptive Optics,,[1] spells out the desired properties for the next generation of detectors for wavefront sensing: very fast, very low noise, and many pixel elements. Specific goals cited were 512 x 512 arrays with 1 kHz frame rates, 1-3 electrons noise per pixel and optical/infrared quantum efficiencies (QE) > 80%. Currently, most array-based wavefront sensor (WFS) detectors are silicon charge coupled devices (CCDs) which can achieve the QE goal but currently have readout schemes that are incapable of simultaneously achieving fast frame rates and low readout noise. For example, the Palomar AO wavefront sensor detector (EEV39 CCD 64 x 64 pixels) can run at frame rates of 1100 Hz at 7.5 e^- rms noise or 50 Hz at 3e^- rms noise[2].

In a CCD, the charge generated by the photon flux at each pixel is transferred to a high gain, low noise amplifier to create an analog voltage for digitization. The noise associated with this amplification increases at faster clocking rates. A typical read noise for 1 MHz clocking rates is ~5 e- noise rms. Scaling from these numbers, a 32 x 32 CCD could be read out in 1 millisecond at a 1MHz pixel rate. So to read out an array of 512 x 512 would require effectively 256 CCD readouts in parallel. And to reduce the noise by a factor of two, the bandwidth would have to be reduced by a factor of 4, resulting in 1024 CCD type readouts to achieve the frame rate goals of the AO roadmap, given current amplifier technology.

A recent new CCD technology is the "Low Light Level,, CCD (L3CCD) by E2V Technologies. It uses a special serial shift register that amplifies the pixel charge at every pixel transfer *before* the output preamp, resulting in output gains of up to 1000 e^- per input photon, easily overwhelming the few electron readout noise of the amplifier. Unfortunately, this amplification process in the shift register is not a noiseless process, and at the higher gains, the variance of the signal charge doubles[3]. So to achieve the same shot noise limited signal to noise ratio, you would have to collect twice the number of photons. Also, for the larger CCDs (E2V 97 512x512) the maximum readout rate is 10MHz corresponding to 40 frames/sec.

An alternative to charge integrating arrays are photon counting detectors. Each photon is detected and registered as one count, and hence, no "read noise,,. Examples in the UV and optical include avalanche photodiodes (APDs) and imaging MCP detectors. Silicon based APDs are fast and have the high QE of silicon in the optical and near IR but are not yet incorporated in large arrays. Imaging MCP detectors can have large area (100 x 100 mm), high spatial resolution (20 μm FWHM), low background dark count, and event timing resolution less than 1 nanosec[4]. Their QE is determined by the characteristics of the photocathode material that absorbs the initial photon and releases the photoelectron. The QE of these photocathodes is now approaching 50%, in particular GaAs and GaAsP (Fig. 11).

*jvv@ssl.berkeley.edu; phone 1 510 643 5666

Advancements in Adaptive Optics, edited by Domenico Bonaccini Calia, Brent L. Ellerbroek, Roberto Ragazzoni, Proceedings of SPIE Vol. 5490 (SPIE, Bellingham, WA, 2004)
0277-786X/04/$15 · doi: 10.1117/12.553017

The problem with using this type of MCP detector as a WFS right now it the inherently serial nature of the readout. Most high resolution readout anodes handle photon events one at a time. For example, delay line anodes, which use the time difference of the anode signal traversing across the anode to determine the photon position, can only allow one event on the anode at a time, otherwise "pileup,, would lead to an incorrect position determination. Delay line lengths of ~50 ns are typical for larger detectors, so even global event rates of 2 MHz result in a 10% pileup fraction, assuming no additional event overhead (ADC conversion, etc). The count rate expected for a strawman Shack Hartman WFS with 5000 lenslets, each focusing to a spot of 1000 events, and updating at 1 kHz rates corresponds to 5000 x 1000 x 1000 = 5 Giga events per second, 3 orders of magnitude faster than some of the fastest imaging photon counters. Clearly some type of integrating detector is required for the WFS application, yet keeping the "noiseless,, operation of a photon counter is very desirable, as it is a crucial characteristic needed for accurate centroid positioning.

Most Shack Hartman WFS image the individual sub-pupils sampled by the lenslet array onto a 2x2 pixel subarray (the "quad cell,,), and use a normalized difference algorithm to measure the centroid of the spot which represents the slope of the wavefront, e.g. $x_{cent} = (A-B)/(A+B)$. However, if the input spot illumination is symetrically shaped with a width on the order of a pixel, then the measured centroid of the input vs. its true centroid is not a linear function of the true position. Furthermore, as the illumination input changes width, the slope of the relationship between measured and true centroid changes. This slope is related to the gain of the feedback to the actuators. So in variable seeing conditions, where the spot sizes are changing, poor phase control can result.

If more pixels are applied to the measurement, this "sampling distortion,, can be substantially reduced. In Fig. 1 are shown simple one dimensional models of various Gaussian width input functions whose measured centroid is plotted against their true input centroid. No read noise or input shot noise was assumed, deviations from linearity are strictly due to the distortions inherent in the assumed sampling algorithm. In the quad cell case (2 samples in one dimension) the non-linearity vs. input centroid position is apparent for a single input width, as is the varying slope for the different widths of the input function. As the number of samples of the Gaussian are increased, (right side of Fig. 1) the non-linearity is decreased as is the sensitivity to width variations. So even with infinite signal to noise ratio, the quad cell can generate errors in the output centroid and therefore errors in the phase determination.

So why do most AO Shack Hartman systems with array detectors use quad cell algorithms? The answer is noise and speed: less pixels mean faster readouts. The centroid variance due to fixed readout noise per pixel for an N x N sampling box scales as N^2 (if the same spatial area is sampled, i.e. the error is in microns, not pixels). If the goal is a centroid determination limited only by the shot noise of the input flux, then more input flux is required to achieve the same SNR. Which of these reasons is dominant must depend on the particular instrument and application (brightness and color of guide star, size and speed of CCD, quality and stability of seeing), but if an array detector with zero readout noise existed and was fast, there would be no hesitation to use more pixels in the centroid determination.

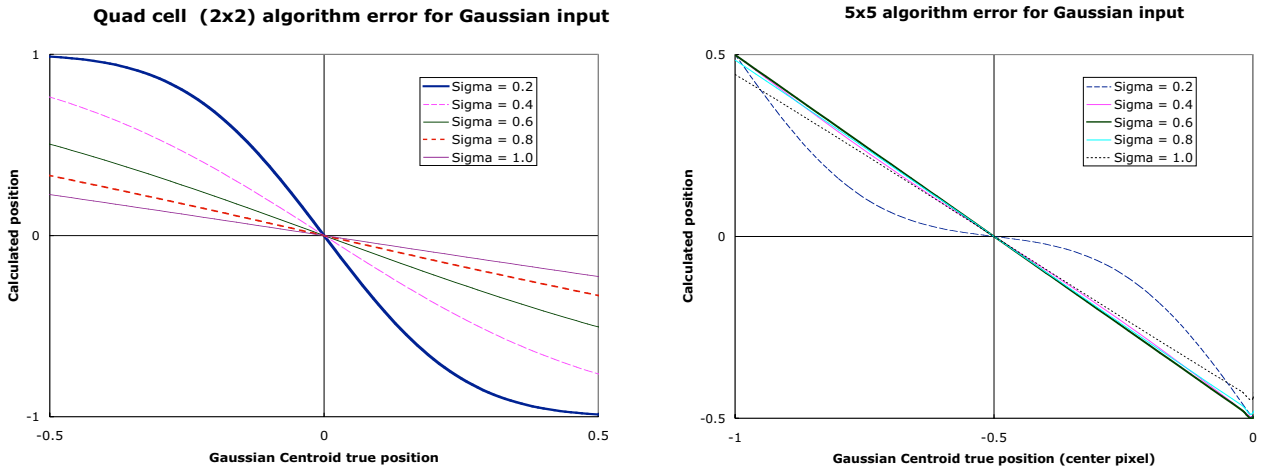

Fig. 1. Model of measured centroid vs. true centroid using pixellated sampling of a Gaussian input function in one dimension. The plotted curves represent different widths of the Gaussian input as a fraction of pixel size and the centroid algorithm is a "center of gravity,, type where x_{cent} is the sum of the used pixel values weighted by the pixel number and divided by the sum of the pixel values. Note the input centroid scales are one pixel wide while the output centroid determinations are different for the two plots. The slope of the quad cell algorithm curves change dramatically with input width while the 5x5 algorithm slopes are similar for different input widths except for the narrowest input function.

Another issue to point out is that for future large area telescopes using laser guide stars, the location of the scattering layer in the atmosphere, whether it be the ~ 100 km of the sodium layer or closer for Rayleigh scattering, will not be in focus, i.e. the wavefront will be curved when a distant astrophysical source wavefront is parallel. This will put most of the Shack Hartman spot images "off null,,, away from the center of the standard quad cell configuration where the non-linearities are greater. More pixels used in the spot sampling results in more accurate and repeatable centroids off null.

2. A NOISELESS, IMAGING MCP DETECTOR AT KHZ FRAME RATES

To take advantage of the noiseless operation of a photon counting detector using MCPs requires a specialized readout that can localize and count the events in a massively parallel way, i.e. pixellated counters. We soon came up with the idea of an idealized application specific integrated circuit (ASIC) pixellated readout behind an MCP in an optical tube with a high QE photocathode. Each 50 x 50 micron pixel of the ASIC would amplify the ~10^4 electrons per photon event into a pulse that would trigger a discriminator which could then be integrated by a counter until read out (and reset) digitally. We envisioned a 512 x 512 array to support 70 x 70 Shack Hartman spots each focused on a set of 5x5 pixels. The count rate per spot from the strawman requirement was 1000 events at 1 kHz or a megahertz, so the maximum rate per pixel would be at most 200 kHz. The array would have to read out in approximately 1 ms. We have been using various ASICs recently to read out cross strips anodes in our high resolution MCP detectors (< 5µm FWHM[4]) that include linear arrays of 128 amplifiers, shapers and discriminators, and realized that such an idealized ASIC would be difficult and expensive to develop on our own. Fortunately, we soon discovered it already existed, being designed and constructed by the Microelectronics Group at CERN for the multi-national MEDIPIX collaboration (http://www.cern.ch/medipix).

Our novel detector scheme should achieve the first three of the specific goals listed above with QEs approaching 40%. The detector (Fig. 2) is a microchannel plate (MCP) image tube with a gallium arsenide (GaAs) photocathode and a new pixellated CMOS readout chip called the "Medipix2,,[5]. Photons interacting with the photocathode release a photoelectron that is proximity focused to the MCP input face. The MCP amplifies this single photoelectron with a gain on the order of 10^4. The resultant charge cloud exits the MCP and lands on the input pad of a Medipix2 pixel where it is counted as one event. The counter will integrate until it is read out in a digital, noiseless process. Also, because the data is digital, it can be read out at ~246 MHz pixel rates, which corresponds to a frame readout time of 266 µs for the current Medipix2 chip.

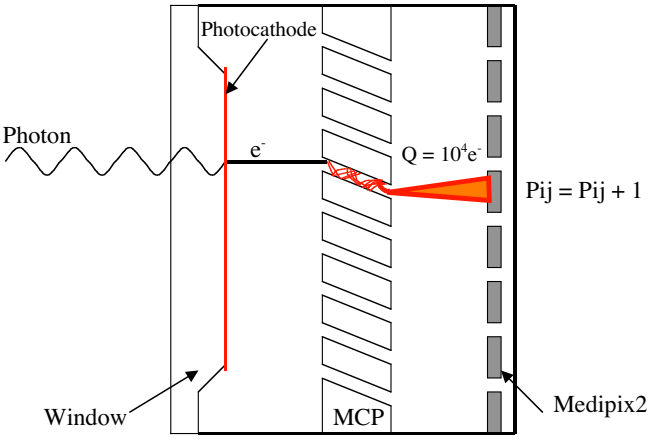

Fig. 2. Schematic of a sealed microchannel plate image sensor. A single photon results in a single count in the pixel Pij. Our scheme uses the Medipix2 ASIC as the readout.

2.1 The Medipix2 ASIC

The Medipix2 chip is a pixel detector readout chip consisting of 256 x 256 identical elements, each working in a single photon counting mode. Each pixel consists of a preamplifier, a discriminator, and a 13 bit pseudo-random counter. The counter logic, based on a shift register, also behaves as the input/output register for the pixel. Each cell also has an 8 bit configuration register which allows masking, testing and 3-bit individual threshold adjust for the discriminator (Fig. 3). It was designed and manufactured in a six-metal 0.25µm CMOS technology. Each 55 x 55 µm pixel contains 508 transistors (Fig. 4). The total active area of the chip is 1.98 cm^2 and is 3-side abuttable to support larger arrays (Fig. 6). Fig. 5 shows the electrical schematic of the Medipix2 layout and how the shift registers relate to the parallel readout.

The input referred noise of the Medipix2 cell has been measured to be ~100 e^- rms and the thresholds can be adjusted to a consistency of ~120 e^- rms.[5] That is why we have baselined an MCP gain of 10^4 e^- per detected photon or a SNR of 100. Note that this noise is in the detection circuit and all we require of the circuit is a minimum of false events. For the minimum threshold setting of 1000 e-, a false trigger would be a 10 sigma noise fluctuation. There is a different style of noise in the amplification process in the MCP as it is statistical in nature, starting with a single photoelectron creating an avalanche of secondaries. At gains of 10^4, the distribution of pulse heights is slightly peaked, but with a finite fraction of events with lower pulse height, so the setting of the thresholds for each pixel will have an effect on the

variation of the sensitivity of the device. We expect this variation to be small (~ 1%) and easily calibrated with high signal to noise flat fields, since the input event rate can be so high.

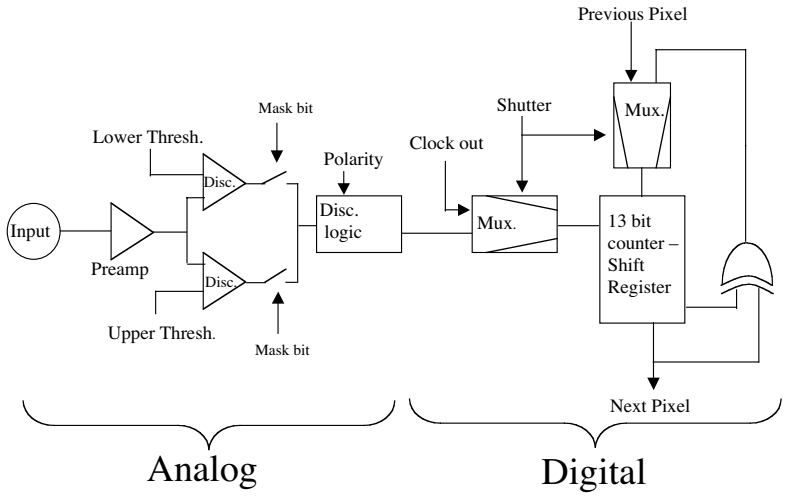

Fig 3. Schematic of major functional blocks in a single Medipix2 pixel. A fast charge event on the input is amplified and shaped by the preamp, discriminated and counted at the shift register (if *Shutter* is disabled). The digital number count is clocked out at high rate through the shift registers of the pixel column when the *Shutter* signal is enabled. Digital configuration bits are input through this same shift register to control thresholds, masking and electrical testing

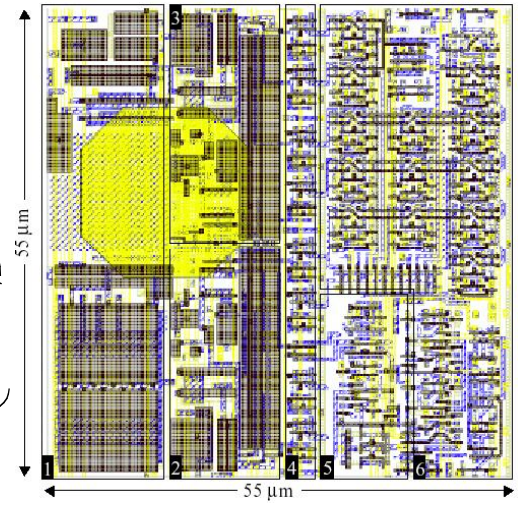

Fig 4. CAD Layout of a single pixel of the Medipix2 ASIC. Amplifier and discriminator are on the left side and the 13 bit shift register is on the right.

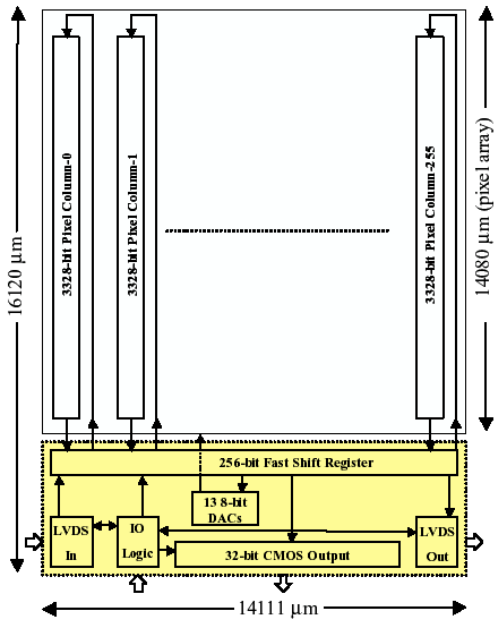

Fig. 5. Schematic of readout architecture of Medipix2 chip organized into 3328 bit columns read out via a 256 bit fast shift register with a 32 bit parallel readout

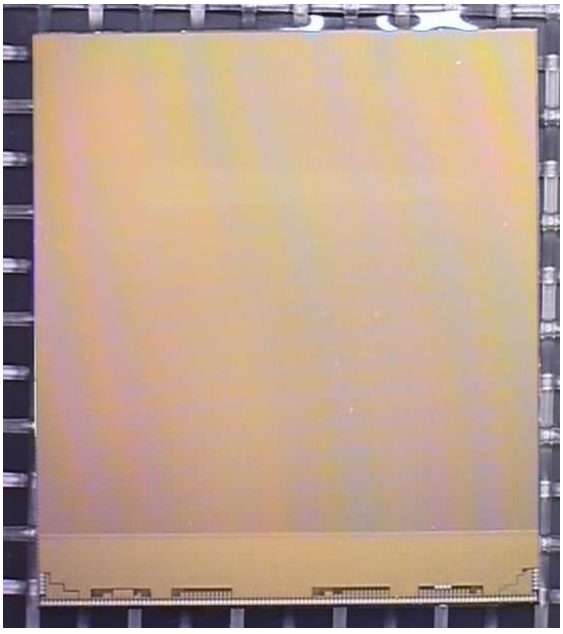

Fig. 6. Image of input face of Medipix2 chip. The dimensions are 1.6 cm high and 1.4 cm wide. The active area has 256x256 pixels and is abuttable on 3 sides.

The Medipix2 has two working modes depending on the *Shutter* input. When the Shutter signal is low, the pixel is in acquisition mode and the discriminator clocks the counter. When the Shutter signal is high, acquisition stops and an external clock is used to shift the data from pixel to pixel out along the columns (Fig. 5). Again note that this is a noiseless process, *digital bits* are being transferred, not charge like in the case of a CCD. For the Medipix2, this has been measured at 80 MHz[6] and modeled up to 100MHz so to read out the whole array will take 266μs. Note that the current design does not allow data collection while reading out, so the 266μs is a fixed deadtime per frame readout. At a kHz rate, the sensor is active 73.4% of time which translates into less sensitivity. This is also true for frame transfer CCDs. For example, a 256x256 frame transfer CCD would take 256μs for the parallel transfer assuming a 1 MHz parallel transfer clock and a mechanical shutter would have to be closed during this time to prevent the input photons from smearing over the columns and increasing the background levels.

The Medipix2 *Shutter* signal can be used as a real electronic shutter with very little deadtime, by not clocking when it is activated. The chip will then ignore input counts by not updating the counter. This ability to gate the input data can prove very useful for AO wavefront sensing of laser guide stars. The sodium scattering region has a ~10 km (varying) depth which results in an extended spot when observed farther away from the laser axis (Fig 7). Chopping or pulsing the laser into 3.3 μs pulses would reduce the projected length of the laser guide star by a factor of ~10 and the *Shutter* signal could be phased to the laser to choose exactly what level in the scattering layer is used. The requirement for a shutter is even more important for a Rayleigh scatter laser guide star as the scattering layer is continuous with height and a shutter is required to choose the acceptance height of the Rayleigh guide star and exclude scattered light from the lower atmosphere. It also would alleviate the need for fast shutters in the optical path such as Pokel's cells. It should be pointed out that there is an additional way to gate our proposed detector by changing the bias voltage of the photocathode with respect to the MCP. This is a standard way of achieving gate timing accuracies at the ~nanosecond level, but the AO requirements are much more easily achieved using this simple digital signal level provided by the Medipix2.

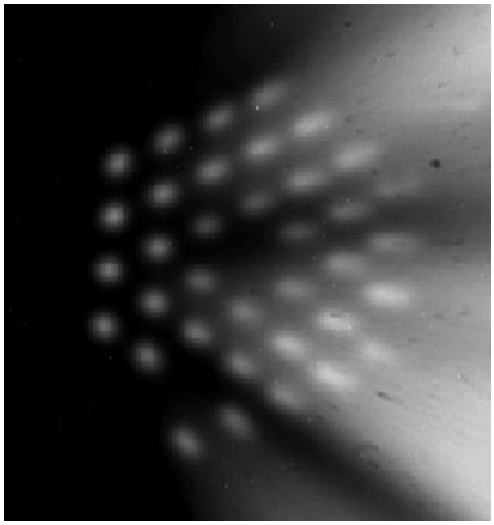

Fig. 7. Images of the Na laser guide star in the Keck SH WFS focal plane showing the parallax across the pupil resulting from observing an illuminated column of emission from the side due to the large size of the telescope. (From Claire Max's AO class 289C, http://cfao.ucolick.org/~max/289C/

The Medipix chips (Medipix1 and Medipix2) were designed at CERN to the specification of the Medipix collaboration, a group of 15 European academic and government labs to improve x-ray and gamma ray imaging for medical, biological and high dynamic range imaging. (For a complete list of the consortium, see: http://web-micfe.web.cern.ch/web-micfe/mic-fe/index.html). We have officially joined this collaboration and were well received as the consortium immediately saw the advantages of adapting the Medipix2 technology to UV and optical imaging, especially in astrophysics. Future development costs for newer versions of the Medipix2 design (mask sets, foundry runs, and readout electronics) are shared among the collaboration. This cost sharing of chip development and production costs is similar to that for scientific grade CCDs for large telescopes.

2.2 MCPs

Microchannel plates consist of an array of holes in a specialized glass substrate whose surface has a high secondary electron coefficient. When biased with a high voltage across the plate, electron(s) entering a pore are accelerated and eventually impact the channel wall, releasing more electrons which continue the process resulting in an avalanche of electrons exiting the rear surface. Typical gains (electrons out/ electrons in) for a single MCP range up to 5 x 10^4 , depending on the voltage applied and the length to diameter (L/d) ratio. A "standard,, MCP might consist of 12μm diameter pores spaced on 15μm centers with hexagonal packing and L/d ratios of 80:1 (1 mm thick). For high resolution imaging using centroiding anodes, gains of 10^6 to 10^8 are usually needed to achieve the high S/N ratios for the analog output signals. This requires either two MCPs in a "chevron,, configuration where the pore bias angle (angle of pore axis with respect to plate normal) is reversed for the second plate with respect to the first, or a "Z-stack,, with 3 MCPs whose bias angles change at the interfaces.

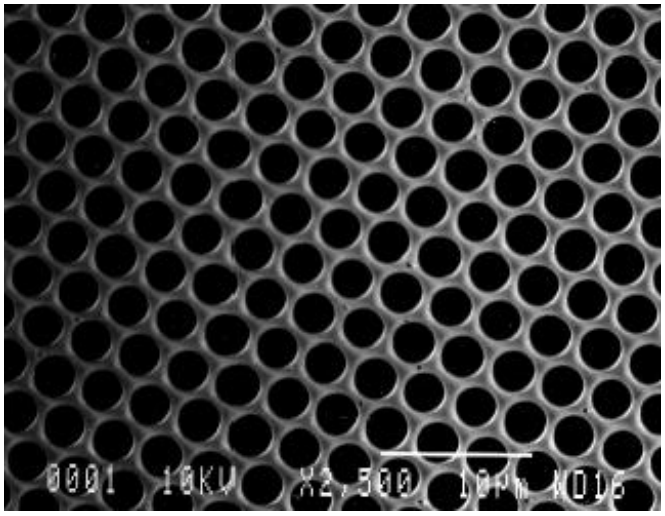

Figure 8. Microscope image of a Burle Industries glass MCP with 2 μm pore diameters and 3μm pore spacing. More pores sampling a given input area result in a higher local dynamic range as each pore has a "deadtime' associated with the recharging of the pores through the local RC network

For a gain of only 10^4, either a single MCP with high L/d ratio or a chevron pair can be used. The advantage of the chevron is that any ions generated in the residual gas of the tube at the MCP output cannot be accelerated back to the photocathode, possibly damaging it. They would be absorbed in the first MCP because of the "bend,, at the interface. Single MCPs are used in phosphor output intensifiers to maintain the highest spatial resolution, since the output charge exits only one channel. In a chevron, the output charge can exit from 3 or more microchannel pores, depending on the phase of the two MCP pore patterns. In the case of our detector, the readout pixels are 55μm square, and pore spacings as low as 3 μm exist (Fig. 8). The pore spacing is more of a concern on how it affects the counting of events at the boundaries of the pixels, leading to the possibility of double counting a single event when the charge cloud impinges on two pixels due to its finite extent. Multi-counting of a single photon event is a blurring term in the image, however, for isolated, multi-photon spots (e.g. a Shack Hartman image), the centroid calculation accuracy is not degraded and depends more on the number of photons detected.

An important new problem faced by this AO detector is the total event rate seen by the MCP(s). There are two issues. One is the gain sag due to the inability of individual microchannels to source more charge than can be replenished given the resistance and capacitance of the microchannel. This has been addressed by new low resistance MCPs now being marketed by the MCP manufacturers (Fig. 9).

Of greater concern is the limited lifetime of the MCP gain due to the internal "scrubbing,, by the high energy flux of electrons in the microchannels changing the structure and chemistry of the secondary electron emitter.[7] This gain degradation initially is fast and then plateaus to a slow but finite amount up to 40 C cm^{-2} (Fig 10). Event rates of 5 GHz at a gain of 10^4 corresponds to a total current of 8 μA. For our 512 x512 strawman detector, the current density would be 1μA/cm^2 and it would take 11520 hours to extract 40 Coulombs of charge cm^{-2} or 960 nights of 12 hours operation on an

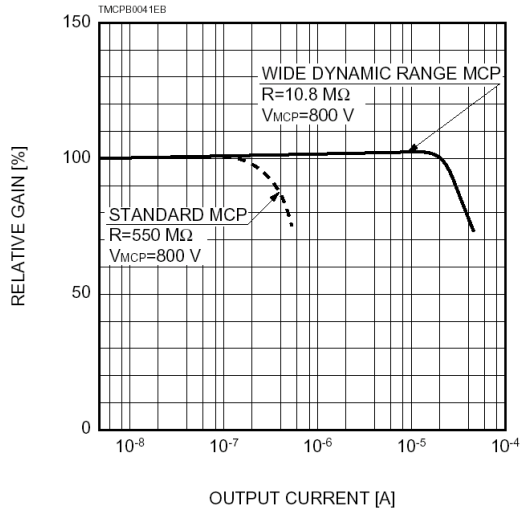

Fig. 9. Plot of MCP gain vs. output current showing gain sag at high input fluxes for two single MCPs, with low resistance and high resistance (http://usa.hamamatsu.com/cmp-detectors/mcps)

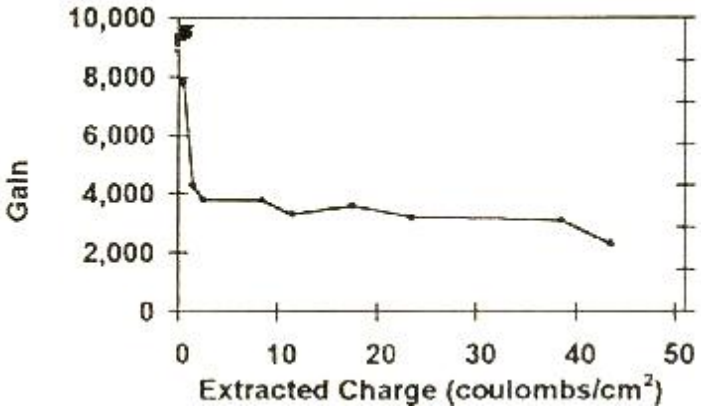

Figure 10. The typical gain degradation of a Burle Industries Long-Life Microchannel Plate as a function of extracted output charge in terms of C cm^{-2}. After an initial burn-in period, in which the detector gain changes as a result of degassing residual gas molecules from the inside of the channel, detector performance is very stable over a large amount of extracted output charge

AO system. Modern image intensifier tubes with single MCPs undergo a preconditioning scrub to get to the gain plateau, and the manufacturers specify lifetimes of 10,000 hours (though they don't quote extraction currents).

2.3 High QE photocathodes in the optical

Imaging, photon counting detectors have been the detectors of choice for EUV and UV astronomy for ~20 years. Optical astronomy has been reluctant to adopt this technology because of the lower quantum efficiency of previously available optical photocathodes compared to bulk silicon. The key issue to apply this detector to AO work is to achieve high quantum efficiency, which is now possible through recent developments of GaAs type photocathodes.

In the near UV/optical part of the spectrum, microchannel plate based sensors generally use multialkali or other environmentally sensitive cathodes deposited onto an input window. Thus they are all built into vacuum tubes constructed to seal and maintain vacuum levels of 10^{-8} Torr or better. A photon impinging on a photocathode in a vacuum tube is converted into a single electron. This photoelectron is multiplied by a MCP stack and registered by a position sensitive electronics readout anode. Various materials can be used as photocathodes to provide optimal sensitivities to different wavelength ranges (Fig. 11).

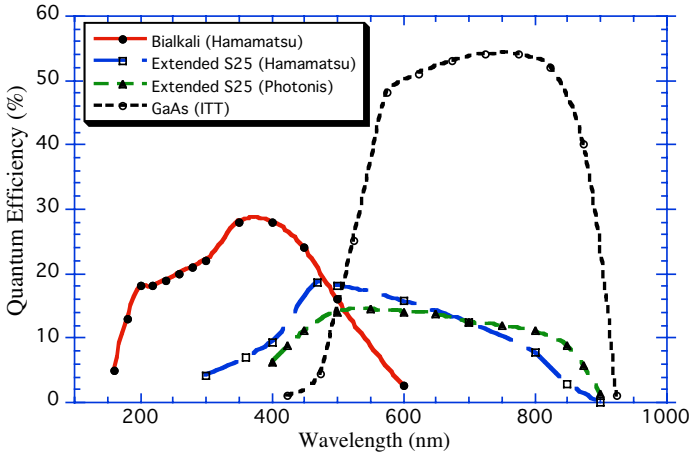

Fig. 11. Quantum efficiencies for commonly used optical regime photocathodes (Sources: www.ittnv.com, www.hamamatsu.com), and the more recent GaAs advances[11].

Application of a photocathode material either as a semitransparent layer on the sensor entrance window or as an opaque layer on a substrate are standard techniques for detection of optical light. In the UV regime ,the application of a photocathode directly on top of a MCP[8] in order to increase its quantum detection efficiency is now standard practice. Our recent work[8,9,10] has expanded the number and type of efficient UV photocathodes and increased the knowledge of how these cathodes behave.

2.3.1 GaAs Photocathodes

Typical cathodes (semitransparent) for the optical/NIR such as bialkali, and multi-alkali are somewhat difficult to produce and require ultrahigh vacuum (<10^{-8} Torr). The best multi-alkali S20 and S25 photocathodes (semitransparent) produced have ~10% to 15% QE at 600 nm (Fig. 11) which is not adequate for AO applications. GaAs photocathodes have been used extensively for a number of years, mainly in night vision applications as the photocathode for Generation III image intensifiers. During that time many advances in performance have been achieved. As demonstrated in Fig. 11, quantum efficiencies in excess of 50% can now be achieved from 550nm to 850nm making them very attractive for astronomical applications. Production of reliable GaAs photocathodes is expensive to implement, so working with an established volume production facility is important.

The number of events generated by thermal electron emission is high for GaAs photocathodes at room temperature (Fig. 12) but at the ~kHz frame rates discussed, the background counts per pixel per frame is close to zero (100 cts per frame over 65k pixels). If, however, the rates in our detectors prove higher than Fig. 12, it is quite acceptable to cool the devices. The data shows that GaAs photocathodes can have backgrounds comparable to multialkali

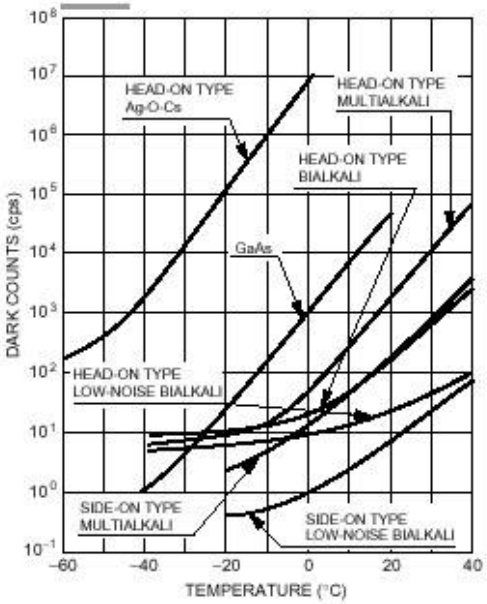

Fig. 12. Dark counts as a function of temperature for various photocathodes. (Source: Hamamatsu.com data sheet)

photocathodes at temperatures below –20 °C. This is less stringent than cooling (-50 °C) for high sensitivity CCD's and can be easily achieved with commercially available Peltier type thermo-electric coolers. The background levels achieved are about 10 events/sec across the whole detector, which is comparable with the noise rate generated by the MCP's (< 5 cps), and considerably less than Si APD's (~ 500 cps per pixel @-20 °C). Thus the background levels for imaging devices using GaAs with modest cooling should be significantly better than other detectors. Given the complexities of cooling and condensation control, running at room temperature would be preferable, and Fig 12 indicates that acceptable background levels are produced at room temperature without significant penalty to a high rate AO system.

2.3.2 Imaging, photon counting detectors with GaAs photocathodes

GaAs photocathodes are commonly used in MCP image intensifiers with a phosphor screen output which have to be readout with another imaging detector like CCDs, incurring the penalty of read noise and speed. Issues of importance for AO applications include cathode lifetimes, sealed tube cleanliness, and MCP barrier layers. The GaAs activated surface is very sensitive to contaminants and early devices had very limited lifetimes. This issue has been addressed by using stringent cleaning processes and using getter pumps inside the sealed tubes. However, most tubes until recently have employed a thin barrier layer applied over the MCP holes to prevent ion feedback from destroying the GaAs. Ion feedback occurs when residual gas, or adsorbed gas in the MCP, is ionized and accelerated back towards the photocathode. Typical image tubes use one MCP so there is no impediment for ions created to travel back to the photocathode. Of course the barrier layer also causes a significant reduction in the QE of the device by stopping some photoelectrons (30%+). Recently, tubes without barrier films have been successfully made as a result of stringent electron flux "scrubbing,, of the MCP's and better tube preparation procedures.

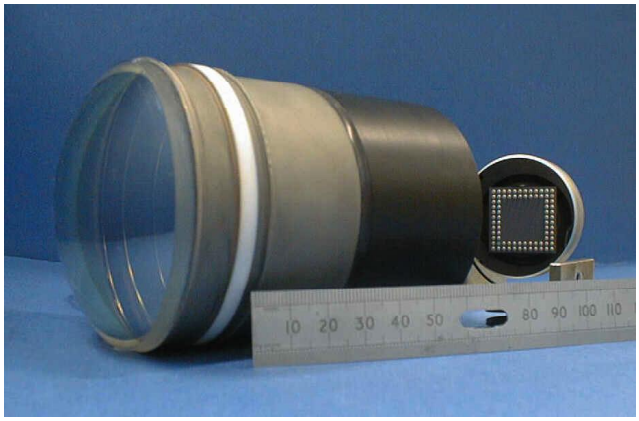

Fig. 13. Photograph of the 72:18 mm HPD prototype tube manufactured by DEP for the LHCb-Ring Imaging Cherenkov (RICH) Detector project equipped with a 61-pixel anode and read out externally with the IDE VA2 analysis chip. (http://www.cern.ch/~gys/LHCb/PixelHPDs.htm)

Our experiences have shown that extreme cleanliness precautions in tube construction result in considerably extended tube lifetimes (decades), though they were intended for scientific applications at relatively low fluxes. In addition we normally require a 3 MCP stack to achieve the gain necessary for single photon counting. This provides an ion feedback barrier at the interface between each MCP (pore bias angles provide a ~26° bend at each interface). We typically do not see any ion feedback effects in our tubes when running at nominal event rates of >100,000 events/sec. Night vision intensifiers usually operate at much higher flux levels with single channel plates and routinely last more than 10,000 hours. One other critical issue is the cleanliness of the readout anode, which is part of the reason that GaAs tubes with position readouts have not been previously developed. The Medipix2 chip has not been integrated into a sealed tube and possibly cannot be heated to the standard tube processing temperatures (~350°C) for extended lengths of time. However, there are special techniques for incorporating modern silicon chips into vacuum tubes. Fig. 13 is a UV phototube fabricated by DEP with a coarse pixellated anode chip fabricated by the Microelectronics Group at CERN. Other examples include electron bombarded CCDs built by Intevac Inc [http://www.intevac.com/mil_imaging].

One other issue affects the quantum efficiency of the final sensor system. The electron detection efficiency of MCP's is approximately equal to their open area ratio of ~70%. So for the final devices the quantum efficiency is about 70% of the cathode efficiency. For the current generation of GaAs this would imply sensor efficiencies of ~30% to ~38%, which is not as high as the 60-70% efficiencies for typical observatory based CCD's, but still very effective for the fast frame rate mode of operation.

3. PRELIMINARY RESULTS AND FUTURE PLANS

We have been funded for a three year program to produce these noiseless, fast imaging detectors and test them in an existing AO WFS on a telescope. In the first year (2004) we have acquired Medipix2 chips and associated readout electronics and are testing them with our laboratory UV MCP detector systems in vacuum. Concurrently, we are

designing the back end mounting scheme for the Medipix2 in consultation with tube vendors. The second year's efforts will involve the actual construction of GaAs tube prototypes and extensive laboratory testing of the same. In the third year we will bring our tubes to the new Laboratory for Adaptive Optics at University of California, Santa Cruz for extensive AO WFS imaging tests before proceeding to Lick observatory for field tests on a working AO WFS.

3.1 Initial Medipix2 readout tests with MCPs

Our first set of Medipix2 chips came mounted on a printed circuit board used for testing by the Medipix collaboration. The board has space for bypass capacitor and resistors and a 68 pin connector. For the eventual vacuum tube application, these parts and connector would be incorporated behind the tube, mounted externally and coupled to the Medipix2 through hermetic feedthroughs. We also designed an MCP detector body that could hold 1 to 3 MCPs at various heights above the Medipix2. The spatial extent of the charge cloud at the Medipix2 input surface is directly proportional to this distance. We could not make this gap smaller than 300μm as the electrical connection to the Medipix chip is through bonding wires on the input surface. There is a voltage bias across this gap to accelerate the electron charge cloud to the Medipix2 to minimize charge spreading. We could also adjust independently the voltage across the MCP(s) to vary the single event gain (previously calibrated with a simple copper anode). This detector assembly was mounted to a 10 inch vacuum flange mounted on a vacuum chamber and actively pumped down to a pressure of 10^{-6} Torr. We used a Hg pen-ray lamp to illuminate the bare MCP and could adjust the lamp intensity to get 10 counts sec^{-1} to 500 million counts sec^{-1}.

The Medipix2 chip was controlled and read out using the "MUROS2„ control electronics developed for the Medipix consortium by the NIKHEF group[12] and the control software "Medisoft Ver. 4.0„ developed by Univ. of Naples Federico II.[13] The actual chip we tested first was designated H4 and its initial settings for preamp gain/bias were done at the Univ. of Geneva. The only extensive optimization of the Medipix2 settings at Berkeley involved the equalization of the pixel lower charge thresholds per the techniques discussed in reference #6.

The initial results shown below are from a chevron set of two, 33 mm diameter Photonis MCPs, 10 μm channel diameter on 12μm centers, 40:1 L/d thickness, and low resistance (22 MΩ per plate). The output end-spoiling was 2 channel diameters. For a bias of 1430V across the two plates, the average gain was 20,000, and we tested up to a gain of 200,000 (1680V). The rear field between the output of the MCPs and the Medipix2 could be varied from 0 to 1600Volts. At the low gains that we operated the MCP, the lamp brightness for full field illumination did not much matter, as we could use the shutter to take very short exposures of a few microseconds to see single photon events or integrate for many seconds to acquire very deep flat fields.

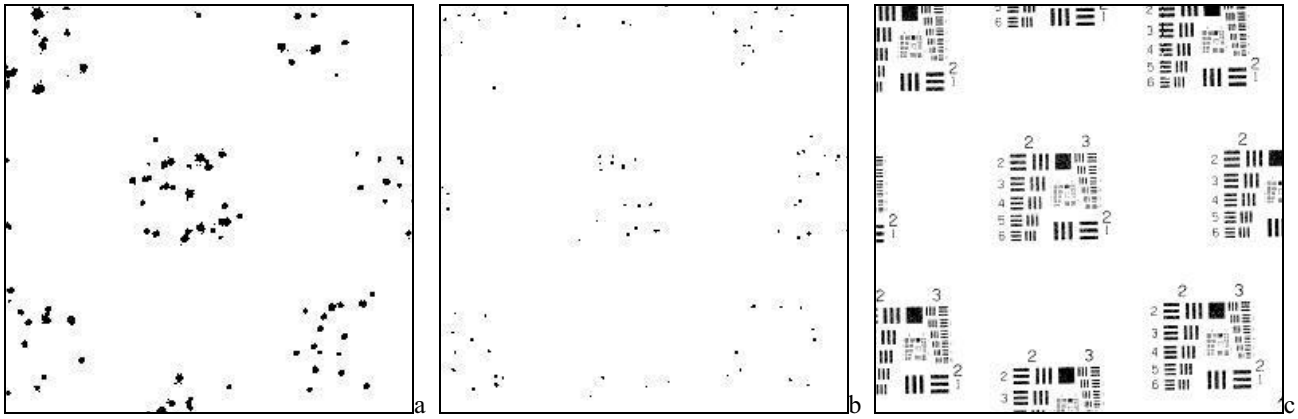

Fig 14. Three single frames of MCP-Medipix2 output: **a)** short integration (100μs) of high gain and low rear field (200k, 300V respectively) showing single photon event spots of extended pixel dimensions due to the large size of the charge cloud and the low charge threshold (~3 kiloelectrons) of the pixel amplifiers. White areas have zero counts. **b)** in contrast to **a**, this short 100 μs integration has a lower gain and a higher rear field (50k, 1500V) with very small photon spot sizes, the average area of which is 2.4 pixels. **c)** a long integration (100s) with the same bias voltages as b, revealing the Air Force test pattern mask. This image is now a gray scale, the counts in each pixel representing the number of photons detected by that pixel.

Figure 14 shows two short and one long integration which contrasts the different data collection modes. The first two are both short enough to see individual photon events coming from the MCP. For the higher gain, lower rear field case (a) , the charge clouds are large and extensive enough to trigger many pixels, each recording 1 count (except for event overlaps, where pixels might count 2 events). By lowering the gain and increasing the rear field (b) , the single photon events trigger, on average, 2.4 pixels and have many less overlapping events at this input rate and integration time. Keeping the same settings as b, image c is a long integration where individual events are no longer distinct. This image reveals the Air Force test pattern (AFTP) mask we mounted on the input surface of the MCP. Pattern 3-2 is just distinguishable (Fig. 15), corresponding to a resolution of 9 lp/mm, exactly the Nyquist limit of a 55µm pixel device.

We have also taken deep flat fields at very high input rates of over 500 million events sec^{-1}. Fig. 16 is a half-second integration at a gain of 20,000 and a rear field of 1600V. The overall uniformity of the flat field is better than 20% with local variations discernable at the locations of known MCP dead spots (white is zero) and MCP multifiber boundaries, features typical in imaging MCP detector flat fields.

Our initial tests probed the extremes of the parameter space for optimizing the detector for AO performance. Future tests of the MCP/Medipix2 interaction will investigate the physical distribution of the charge cloud as a function of the adjustable detector parameters including gain, rear field, MCP-Medipix2 gap spacing, and MCP end spoiling. We will also investigate the performance of MCPs with different L/d ratios and channel diameters. Given the knowledge of the charge cloud spatial distribution, we can model the expected spatial resolution and the centroiding accuracy of Shack Hartman spots.

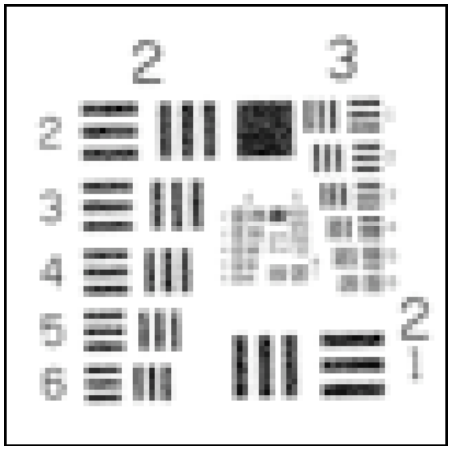

Fig. 15. Zoom of center of Fig. 14c showing the 3-2 limit (9lp/mm) of spatial resolution of the 55µm Medipix2 pixel

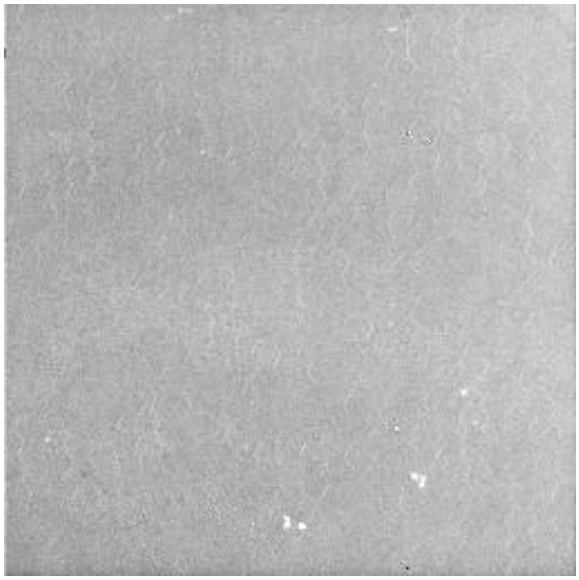

Fig. 16. Flat field of MCP-Medipix detector using UV light. Note MCP features such as the dead spots and the multifiber hexagonal boundaries.

3.2 GaAs measurements and sealed detector design

At the end of the initial MCP-Medipix2 tests, we will have the data needed for the design of the optical tube: MCP pore spacing, thickness and number, minimum gain, maximum count rates, MCP-Medipix2 spacing and voltage bias. We then will proceed to the design of the tube back end that holds the Medipix2 anode with hermetic vias to get the signals in and out of the vacuum tube.

Several steps are necessary to successfully integrate our image readout system into a GaAs cathode tube. An important task is derivation of the design and construction flow of the sealed tube development. We have assumed that we will use the basic design provided by the existing 18mm format GaAs tubes offered by tube vendors. From a cost and schedule standpoint this is an essential strategy. We will then provide an ASIC readout and mounting structure that will form the replacement for the current anode technologies without requiring significant changes to their tube process tooling. This must also be done in such a way as to not prevent the correct thermal and vacuum processing of the GaAs

photocathode or of the final seal of the cathode/window to the sealed tube body. At the same time we must keep the ASIC below its thermal limit while ensuring its cleanliness.

To develop a GaAs sealed tube the design of the Medipix2 anode must be compatible with the standard 18mm tube configuration. The use of 18 mm GaAs tube design limits us to one Medipix2 chip with a 256 x 256 readout. Scaling up to a 512 x 512 tube with four Medipix2 chips abutted is beyond the scope of this project, and logically should await this demonstration of its feasibility. The Medipix2 will be mounted on a customized flange to accommodate the tube seal and required electrical characteristics. Most likely the flange will be laser welded to the bottom of a standard tube body. Photoelectrons emitted from the cathode are accelerated over a ~ 300 μm gap to the MCP stack. The MCP's should be two 25 mm, 40:1 length-to-diameter ratio (L/d) (gain ~ 10^4), low resistivity (< 50MΩ) MCP's which we will specially procure so that the local event recovery times are short. The image tube(s) will then be processed at the tube vendor including the vacuum bake and MCP scrub, and sealed with a high QE GaAs cathode of standard time response. After a successful tube seal we will proceed to evaluate the device by measuring the gain, background (now cathode dominated), QE, spatial resolution and uniformity, local and global event rate processing capability, and timing resolution with the system electronics.

3.3 Adaptive Optics Tests

Though our facilities at the Space Science Lab have the ability to measure optical QE and project images onto the detector, we do not have the sophisticated optical resources to mimic an AO system or aberrated wavefronts. We plan to use the facilities of the new Laboratory for Adaptive Optics (LAO) at U.C Santa Cruz, whose charter is to develop adaptive optics techniques for extremely large ground-based telescopes and test and evaluate new components/technologies as they become available. Their facilities can scale down a 30 m primary mirror and 40 km of atmosphere onto the lab bench. They have a laser guide star simulator, including sodium layer height (elongation), AO relay optics, deformable mirrors, atmospheric phase aberration plates and various wavefront sensors. We plan to run a full array of AO tests in consultation with the LAO staff, to demonstrate the effectiveness of the imaging tube as the detector for wavefront sensing.

The initial tests will be done "open loop,, to characterize the detectors response while varying the input illumination wavefronts. The detector will then be calibrated to the wavefront re-constructor, first using a quad cell type algorithm and then with a full 5x5 pixel centroiding algorithm. Once the detector and reconstructor are matched and tuned, closed loop testing can begin. We will perform some of our tests at the kHz rates if the LAO equipment can support this bandwidth.

If we are successful in our laboratory tests, we expect to be invited to try the detector(s) on the AO system at Lick Observatory. Ultimately, the goal of this project is to demonstrate the use of the noiseless, kHz frame rate image tubes in AO wavefront sensors on working telescopes. We can then measure closed loop performance parameters such as Strehl ratio, sensitivity to both laser and natural guide stars, stability and background, and compare this performance to existing WFS detectors. We would also like to demonstrate improved performance by taking advantage of the lower noise, more pixels, higher frame rate, and gateable integration of the Medipix2 readout. Since this detector architecture is novel to the optical and infrared astronomical communities, it is imperative that we demonstrate its performance at a telescope AO system and disseminate the results widely through publications and talks at astronomical conferences.

Future advances in optical photocathode, MCP and readout ASIC technologies could all be incorporated in advanced versions of the noiseless tube. Silicon MCPs[14] hold the promise of better spatial uniformity with coherent hole patterns, longer lifetime and higher counting rates. They also can have larger open area ratios, resulting in a higher QE to the input photoelectron. The Medipix2 ASIC was not optimized for AO, so there are a number of enhancements that could be made to the chip, even without the technological advancements expected from CMOS fabrication processes. Larger formats can be obtained by abutting the chips. Faster frame rates can be increased by faster downstream electronics and adding more digital readout channels in parallel. Smaller pixel sizes must await higher transistor densities. However, based on the history of minimum lithography feature size, the wait will not be long.

ACKNOWLEDGMENTS

The authors wish to thank the Medipix Collaboration for the Medipix2 chips, readout hardware and software and for valuable advice. This material presented here is based upon work supported by AURA through the NSF under AURA cooperative agreement # AST-0132798-SPO#6(AST-0336888)

REFERENCES

1. Angel, R. et al “A Roadmap for the Development of Astronomical Adaptive Optics “, July 6, 2000, http://www.noao.edu/dir/ao/
2. DuVarney, R., Bleau, C., Motter, G., Dekany, R., Troy, M., Brack, G., "SciMeasure Wavefront Sensor Cameras and their Application in the Palomar Adaptive Optics System", Experimental Astronomy, 11, 237, 2001
3. Mackay C. D., Tubbs R. N., Bell R., Burt D. J., Jerram P., Moody I., “Subelectron read noise at MHz pixel rates,,, SPIE, 4306, 298, 2001
4. Siegmund O. H. W., “Advances in microchannel plate detectors for UV/visible astronomy,,, SPIE, 4854, 190, 2003
5. Llopart, X., M.Campbell, R.Dinapoli, D.SanSegundo, E.Pernigotti, “Medipix2, a 64k pixel readout chip with 55 μm square elements working in single photon counting mode,,, IEEE Trans. Nucl. Sci. NS-49 (2002) 2279
6. Llopart X. and M. Campbell, “First test measurements of a 64k pixel readout chip working in single photon counting mode,, Nuclear Instruments and Methods in Physics Research Section A: Volume 509, Issues 1-3, 21 August 2003 ,Pages 157-163
7. Fraser, G.W., IEEE Trans. Nucl. Sci. NS-35, 529, (1988)
8. Siegmund O. H., Gummin M. A., Sasseen T., Jelinsky P. N., Gaines G. A., Hull J., Stock J. M., Edgar M. L., Welsh B. Y., Jelinsky S. R., Vallerga J. V., Microchannel plates for the UVCS and SUMER instruments on the SOHO satellite, SPIE, 2518, 355, 1995
9. Tremsin, A. S., and Siegmund, O. H. W., “The dependence of quantum efficiency of alkali halide photocathodes on the radiation incidence angle,,, Proceedings of the SPIE 3765:441-451. 1999
10. Tremsin, A. S., and Siegmund, O. H. W., , Polycrystalline diamond films as prospective UV photocathodes, Proceedings of the SPIE 4139, 2000
11. Smith, B., K. Passmore, A. Smith, R. Lundberg, et al, 2003, NIM Phys. Res. A, 504, 182-187.
12. Bello, David San Segundo , Martin van Beuzekom, Peter Jansweijer, Hans Verkooijen and Jan Visschers “An interface board for the control and data acquisition of the Medipix2 chip,,, Nuclear Instru. and Meth. in Physics Research Section A:, Vol 509 Pages 164-17 , 2003
13. Bertolucci, E., Conti, M., Mettivier, G, Maiorino, M. ,Montesi, M. C. and Russo, P. “Medisoft4: A software procedure for the Medipix2 readoutchip,,, in. IEEE Nuclear Science Symp. Medical Imaging Conf., San Diego, CA, Nov. 2001.
14. Tremsin A. S., Vallerga J. V., Siegmund O. H. W., Beetz C. P., Boerstler R. W., The latest developments of high-gain Si microchannel plates, Proccedings of the SPIE, 4854, 224, 2003